AD_____

AWARD NUMBER: W81XWH-05-1-0363

TITLE: Miniature and Molecularly Specific Optical Screening Technologies for Breast Cancer

PRINCIPAL INVESTIGATOR: Nimmi Ramanujam, Ph.D.

CONTRACTING ORGANIZATION: Duke University
Durham, NC 27708

REPORT DATE: October 2009

TYPE OF REPORT: Annual

PREPARED FOR: U.S. Army Medical Research and Materiel Command
Fort Detrick, Maryland 21702-5012

DISTRIBUTION STATEMENT: Approved for Public Release;
Distribution Unlimited

The views, opinions and/or findings contained in this report are those of the author(s) and should not be construed as an official Department of the Army position, policy or decision unless so designated by other documentation.

REPORT DOCUMENTATION PAGE

Form Approved
OMB No. 0704-0188

Public reporting burden for this collection of information is estimated to average 1 hour per response, including the time for reviewing instructions, searching existing data sources, gathering and maintaining the data needed, and completing and reviewing this collection of information. Send comments regarding this burden estimate or any other aspect of this collection of information, including suggestions for reducing this burden to Department of Defense, Washington Headquarters Services, Directorate for Information Operations and Reports (0704-0188), 1215 Jefferson Davis Highway, Suite 1204, Arlington, VA 22202-4302. Respondents should be aware that notwithstanding any other provision of law, no person shall be subject to any penalty for failing to comply with a collection of information if it does not display a currently valid OMB control number. **PLEASE DO NOT RETURN YOUR FORM TO THE ABOVE ADDRESS.**

1. REPORT DATE	2. REPORT TYPE	3. DATES COVERED
1 October 2009	Annual	1 Sep 2008 – 31 Aug 2009

4. TITLE AND SUBTITLE

Miniature and Molecularly Specific Optical Screening Technologies for Breast Cancer

5a. CONTRACT NUMBER

5b. GRANT NUMBER
W81XWH-05-1-0363

5c. PROGRAM ELEMENT NUMBER

6. AUTHOR(S)

Nimmi Ramanujam, Ph.D.

E-Mail: nimmi@duke.edu

5d. PROJECT NUMBER

5e. TASK NUMBER

5f. WORK UNIT NUMBER

7. PERFORMING ORGANIZATION NAME(S) AND ADDRESS(ES)

Duke University
Durham, NC 27708

8. PERFORMING ORGANIZATION REPORT NUMBER

9. SPONSORING / MONITORING AGENCY NAME(S) AND ADDRESS(ES)
U.S. Army Medical Research and Materiel Command
Fort Detrick, Maryland 21702-5012

10. SPONSOR/MONITOR'S ACRONYM(S)

11. SPONSOR/MONITOR'S REPORT NUMBER(S)

12. DISTRIBUTION / AVAILABILITY STATEMENT
Approved for Public Release; Distribution Unlimited

13. SUPPLEMENTARY NOTES

14. ABSTRACT
The goal of this proposal is to harness the power of light to create "miniature and molecularly specific optical technologies" for breast cancer diagnosis and detection. The miniature technologies will leverage on millimeter scale silicon detectors and LEDs to make compact devices that can be used in a practical clinical setting for breast cancer detection. The features that will be exploited for optical detection/diagnosis of breast cancer will include the physiological, structural and molecular alterations that accompany the transformation of a cell from a normal to malignant state. This proposal also focuses on using contrast agents, specifically aminolevulinic acid (ALA) induced protoporphyrin IX (PpIX) and NBDG, for the molecular detection of breast cancer.

15. SUBJECT TERMS
optical, spectroscopy, imaging, fiber-optic, molecular, screening

16. SECURITY CLASSIFICATION OF:			17. LIMITATION OF ABSTRACT	18. NUMBER OF PAGES	19a. NAME OF RESPONSIBLE PERSON
a. REPORT	b. ABSTRACT	c. THIS PAGE			19b. TELEPHONE NUMBER *(include area code)*
U	U	U	UU	19	USAMRMC

Table of Contents

1. INTRODUCTION

The objective of this proposal is to harness the power of light to create “miniature and molecularly specific optical technologies” for the eradication of breast cancer. Specifically this application focuses on a system on a chip device to detect molecularly specific sources of optical contrast for breast cancer. Both intrinsic (hemoglobin saturation, total hemoglobin content, reduction-oxidation ratio) and extrinsic sources of optical contrast (specifically aminolevulinic acid (ALA) induced protoporphyrin IX (PpIX) and 2-[*N*-(7-nitrobenz-2-oxa-1,3-diazol-4-yl)amino]-2-deoxy-D-glucose (2-NBDG) will be studied for breast cancer imaging. These sources of contrast coupled with the system on a chip device will be initially used for intraoperative margin assessment and predicting/evaluating response to therapy. . Once we have established the feasibility of using this technology in the margin assessment and therapy application, we will focus on applications that focus on early detection, including core needle biopsy and ductoscopy, which require further modifications to the technology.

2.1 Project 1: System-on-a-chip device

A. Original SOW for five years

1) *To establish the design specifications of the first-generation system-on-a-chip device.* This aim will involve throughput calculations and Monte Carlo modeling to determine the signal-to-noise ratio that can be achieved with the nano scale sources and detectors, and the experimental evaluation of the signal-to-noise of the test system on turbid “tissue-like” media. The signal-to-noise ratios achieved with the test system will be quantitatively compared to that achieved with a standard bench top system (year 1).

2) *To engineer and test the first-generation system-on-a-chip device.* The knowledge base derived from aim 1 will be used to engineer a first generation system-on-a-chip device and the performance of the device will be characterized on synthetic tissue phantom models. The signal-to-noise ratio and fluorescence attenuation characteristics of the system-on-a-chip device will be compared to that of a standard bench top counterpart (year 2).

3) *To experimentally establish the signal-to-noise ratio with which the system-on-a-chip device can measure the fluorescence of ex vivo human breast tissues.* The system-on-a-chip device will be used to measure the fluorescence properties of 25 pair of malignant and non-malignant breast tissues excised from approximately 25 patients undergoing breast cancer surgery. The results obtained from this study will be quantitatively compared to benchmarks established by our bench top counterpart, which has been shown to measure breast tissue fluorescence with excellent signal-to-noise ratio (year 3).

4) *To test the feasibility of implementing optical spectroscopy via a ductoscope.* The system-on-a-chip device will be incorporated into a standard ductoscope. The ductoscope will be used to measure the fluorescence properties of 25 pair of malignant and non-malignant breast tissues excised from approximately 25 patients undergoing breast cancer surgery (years 4-5).

B. Summary of accomplishments in year 1

In year 1, we have completed the main goals of the SOW for year 1. The major achievements include thermal modeling of the heat dissipation effects of compact LEDs on tissue samples, selection of multi-wavelength compact light sources, calculating bandwidth effects of broadband light sources (such as LEDs) on the RMS errors for the extracted tissue optical and physiological properties, selection of photodiodes, and the design and testing of various single-pixel probe prototypes (P1 and P2 as shown in Figure 2.1). The major deviation from the SOW is that we used commercially available light sources and detector in our design, instead of using nano scale sources.

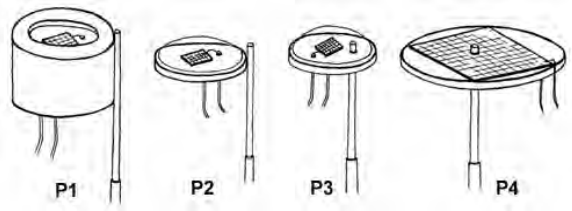

Figure 2.1. Conceptual drawings of four single-pixel probe geometries P1-P4.

C. Summary of accomplishments in year 2

In year 2, we used knowledge base derived from year 1 to build more first generation single-pixel devices using an optical fiber for illumination and photodiodes for the collection of diffusely reflected light from a tissue sample. In particular, we have built single-pixel probes of different illumination and detection geometries named as P3-1 (600 μm fiber), P3-2 (1 mm fiber), P4-1 (600 μm fiber), and P4-2 (1 mm fiber), as shown in Figure 2.1, all using and 2.4 mm photodiode. P3-1 and P3-2 were tested in synthetic tissue phantoms with known optical properties, and their experimental diffuse reflectance spectra were compared with those of a forward Monte Carlo model.

We have also extracted the phantom optical properties from the diffuse reflectance spectra obtained from a tunable light source using an inverse Monte Carlo (MC) model. For P3-2, we found that the overall errors for quantifying the absorption and scattering coefficients were 6.0±5.6% and 6.1±4.7%, respectively. These results are comparable with those achieved with our bench-top system which has an overall error 5.8±5.1% and 3.0±3.1% for extracting μ_a and μ_s', respectively. A short paper on P3-2 has been accepted for publication by the Journal of Biomedical Optics Letters [1] and a copy of the manuscript is attached to this report. Phantom optical properties with reduced number of wavelengths were also extracted and compared to that of the bench-top system with all wavelengths.

In year 2, a clinical study conducted by our group using the bench-top system and the MC model showed that DRS alone has achieved comparable sensitivity and specificity for discriminating malignant from nonmalignant breast tissues as combined reflectance and fluorescence spectroscopy[2]. Therefore, our research in this miniature device has been focused mainly on diffuse reflectance spectroscopy (DRS) for breast cancer diagnosis and tumor margin assessment.

D. Summary of accomplishments in year 3

In year 3, we have modified the probe geometries of the single-pixel probe developed in year 2 in order to increase the signal-to-noise ratio of the probe and to be able to extract a much larger range of optical properties than those of the probes built in year 2. The new probe was tested in synthetic tissue phantoms over a wide range of absorption and reduced scattering coefficients, and the phantom optical properties were extracted from the diffuse reflectance spectra obtained from the tunable light source and new probe with the inverse MC model previously developed by our group. Using the same phantom data collected by our new probe, optical properties with a reduced number of wavelengths were extracted to assess the feasibility of replacing the tunable light source with several smaller LEDs to further reduce the size and cost of the current system. In addition, cross-talk analysis was performed as a first step to multiplex the single pixel system into an imaging system that can quantify tissue physiological and morphological properties over a large tissue area. We have also fabricated a 3x3 fiber-photodiode array for test in the lab.

Although the original goals of the SOW is to use the system-on-a-chip device to measure the fluorescence properties of 25 pair of malignant and non-malignant breast tissues excised from approximately 25 patients undergoing breast cancer surgery, we understand that many challenges exist and it may take a relatively long time to reach this goal. As an intermediate step, the work in

year 3 has been focused on partially miniaturizing the current bench-top system. This miniaturized probe preserves the potential for multiplexing that can be used for spectral imaging of tissue while uses all the wavelengths available to the bench-top system.

In year 3, a poster on the single-pixel device titled "A Miniature Optical Device for Noninvasive, Fast Characterization of Tumor Pathology," was presented to the 2008 OSA Topic Meeting in Biomedical Optics**,** March 16-19, 2008, St. Petersburg, Florida. Manuscripts are also in final preparation for Optics Express and Journal of Biomedical Optics Letters.

E. Progress report for year 4

Revised SOW:

Due to the deviation of the SOW for years 1-3, our research plans on the system-on-a-chip for years 4 were also revised accordingly.

- To complete the construction of the 3x3 multi-pixel system and test it in liquid tissue phantoms.
- To investigate a new xenon light source with a filter wheel for better light coupling between the lamp and the fibers and reduced number of wavelengths in phantom studies.
- To replace the silicon detector with a GaAs detector plate which has improved sensitivity and can be customized for our specific illumination and collection geometry.
- To assemble a first prototype back-illuminated spectral imaging device and construct the electronics box.

(a) Introduction

In year 4, we have made significant progress in each task listed in the revised SOW. First, we have completed the construction of the 3x3 fiber-based illumination spectral imaging array. The 3x3 array was tested in liquid tissue-simulating phantoms using a new xenon light source with eight bandpass filters (simulating reduced number of wavelength). Second , we have built and tested a single-pixel version of the back-illuminated spectral imaging (BISI) probe. The single-pixel BISI probe was expanded to a 4x4 array for spectral imaging. Finally, we have also made initial photodiode arrays using a GaAs technology. With the custom GaAs array and the back-illumination strategy, a miniature spectral imaging system can be built with the application for intra-operative assessment of tumor margins.

(b) Fiber-Illumination Spectral Imaging (FISI) System

System Design

In previous years we have already demonstrated the feasibility of a photodiode-based detection strategy for quantitative optical spectroscopy. Previous work has focused primarily on a single pixel, point measurement system utilizing a photodiode. In year 4, a new compact FISI system, as shown in Figure 2.2A, was constructed to demonstrate scalability of the single pixel photodiode-based probe to an imaging system and further reduction in the cost and size of the system. The FISI system uses a broadband Xe light source with 8 bandpass filters with a center wavelength determined in year 3 (400, 420, 440, 470, 500, 530, 570, and 600 nm). This resulted in a much smaller, cheaper, and simpler system design. A photograph of the distal end of the imaging probe is shown in Figure 2.2B. Each of the 9 illumination optical fibers (0.6 mm core diameter) fed into the center of a square silicon photodiode, forming a 3x3 matrix.

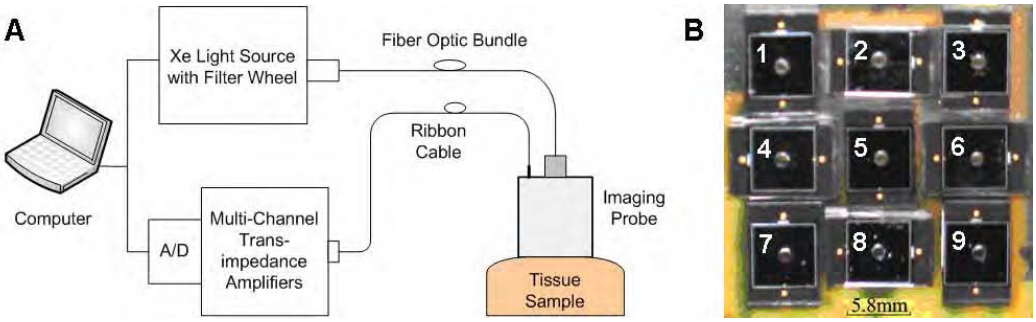

Figure 2.2: The fiber-illumination spectral imaging (FISI) system. A) A system schematic which details the illumination and collection setups. B) Photograph of the tip of the 3x3 photodiode spectral imaging matrix.

System Characterization and Performance

The FISI system was assembled and constructed. The key physical parameters of the FISI system were compared to those of the current clinical spectral imaging system in
Table 2.1. Both the size and cost of the FISI system are significantly reduced compared to the current clinical system. More importantly, the FISI system can be more easily expanded to a larger and denser imaging array with matured semiconductor technology.

Table 2.1: Side-by-side comparison of key physical system parameters between the current clinical system and FISI system. A noteworthy comparison is the large reduction of footprint between the bench-top system and the 3x3 photodiode-Fiber system.

Spectral imaging system	Probe geometry (One channel)		Number of channels	Center-to-Center distance between channels (mm)	Footprint of system (L x W x H) (m)
	Illumination	Collection			
Current Clinical System	**1 mm diameter (19, 0.2 mm fibers)**	**Ring of 4, 0.2 mm diameter fibers**	**8**	**10**	**2 x 1.5 x 1**
Fiber-Illuminated System	**0.6 mm diameter fiber**	**5.8 x 5.8 mm SI Photodiode**	**9**	**8**	**0.35 x 0.3 x 0.2**

Extensive Monte Carlo (MC) simulations were run to evaluate the sensing depth and crosstalk between adjacent pixels and comparisons to the current clinical system. The sensing depth is defined as the depth above which 90% of the photons visited. Any light collected that originated from an adjacent pixel's illumination fiber was considered cross-talk, as it would adversely impact the modeling and inversion accuracy. The optical properties used in the sensing depth simulations were based on clinically measured optical properties of three different breast tissue types (malignant, normal adipose, normal non-adipose) encountered in our clinical measurements. Table 2.2 shows the calculated sensing depth of both the current clinical system and FISI system. The crosstalk shown in Table 2.2 was calculated using μ_a = 0.65 cm^{-1} and μ_s' = 5.97 cm^{-1}, the "worst case scenario" for cross talk (low absorption and low scattering) based on values measured clinically.

Table 2.2: Comparison of simulated data between the bench-top system and the 3x3 FISI system for three tissue types seen in the clinical current study.

Spectral Imaging System	Optical Properties of Three Tissue Types (cm^{-1})	Sensing Depth (mm)†	Cross Talk between Adjacent Pixels
Current Clinical System	**Malignant (M) : μ_a = 23.14; μ_s' = 9.09** **Adipose (A) : μ_a = 9.24; μ_s' = 5.88** **Non-Adipose (NA): μ_a = 9.45; μ_s' = 8.33**	**M: 0.8 – 1.8** **A: 0.7 – 1.7** **NA: 0.5 – 1.4**	**0.0602%**
Fiber-Illuminated System		**M: 0.6 – 1.9** **A: 0.9 – 2.7** **NA: 0.8 – 2.3**	**2.23%**

The signal-to-noise ratio (SNR) of the FISI system was measured on a highly absorbing liquid phantom with optical properties of μ_a = 7.00 cm^{-1} and μ_s' = 14.84 cm^{-1}. The SNR is shown in Figure 2.3A, along with the optical power (measured at 400 nm) at the tip of each illumination fiber in Figure 2.3B. The minimum SNR was about 40 dB (at 400 nm) and the max SNR was 65 dB (at 600 nm). These SNRs are comparable with those obtained with the current clinical system. Pixel 8 was damaged during the construction process, so data was not presented for this pixel.

A

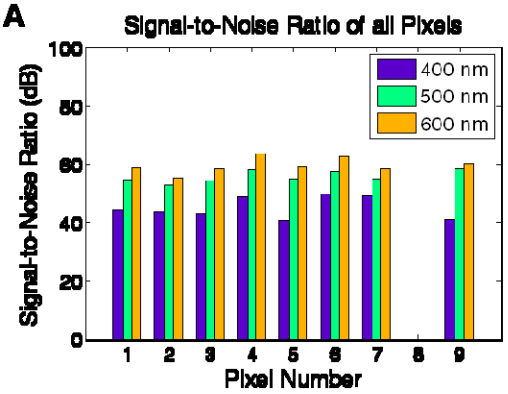

B

Pixel #	Optical Power (μW)
1	700
2	650
3	770
4	720
5	720
6	800
7	500
9	200

Figure 2.3: A) SNR for all pixels at three different wavelengths (400, 500, 600 nm). The SNR was calculated by taking 15 repeated measurements on a liquid phantom and dividing the mean by the standard deviation. The optical properties of the phantom used in the SNR measurements were μ_a = 7.00 cm-1 and μ_s' = 14.84 cm-1. B) The table on the right indicates the optical power output (at 400 nm) from the illumination fiber of each pixel for the SNR measurements.

Tissue Mimicking Phantom Study Results

To test the optical property extraction accuracy and robustness of the FISI system, a tissue mimicking phantom study was designed. The phantoms contained variable concentrations of hemoglobin (Hb) (H0267, Sigma Co.) as the absorber and 1-μm polystyrene spheres (07310-15, Polysciences, Inc.) as the scatterer. The absorption coefficient (μ_a) was determined from a spectrophotometer measurement of a diluted Hb stock solution and the reduced scattering coefficients (μ_s') was calculated using the Mie Theory [3] with known size, density and refractive index of the scatterers. Table 2.3 documents the expected optical properties (μ_a and μ_s') of the 14 phantoms made for this phantom study. The optical property range was chosen to match those of a previous phantom study performed with the current clinical system to enable a direct comparison between systems of optical property extraction accuracy.

Table 2.3: Summary of the optical properties of all 14 liquid phantoms (average value over 400-600 nm) used to test the extraction accuracy of the 3x3 FISI system. The highlighted phantom was used as the reference phantom for the inversions.

Phantom #	1	2	3	4	5	6	7
μ_a (cm^{-1})	0.50	1.00	1.50	2.00	2.50	3.00	3.50
μ_s' (cm^{-1})	20.53	20.09	19.66	19.22	18.78	18.34	17.91
[Hb] (μM)	2.28	4.57	6.85	9.14	11.42	13.71	15.99
Phantom #	8	9	10	11	12	13	14
μ_a (cm^{-1})	4.00	4.50	5.00	5.50	6.00	6.50	7.00
μ_s' (cm^{-1})	17.47	17.03	16.59	16.15	15.72	15.28	14.84
[Hb] (μM)	18.28	20.56	22.84	25.13	27.41	29.70	31.98

To measure the diffuse reflectance of each of these phantoms, the probe tip was placed flush in contact with the surface of the liquid phantom. Each of the 8 available wavelengths was sequentially

launched into the 9 illumination fibers and the diffusely reflected light was measured with all nine photodiodes. Wavelength switching and signal measurement was controlled by a custom LabView program. A separate calibration measurement was taken, after all the phantom measurements, on a Spectralon 99% reflectance standard (SRS-99-010, Labsphere Inc.) with the same measurement procedure and integration time. The collected spectrum of liquid phantom was divided by that of the reflectance standard to obtain the calibrated diffuse reflectance spectrum, correcting for wavelength-dependent instrument throughput and the spectral shape of the source. Figure 2.4A shows a comparison of representative diffuse reflectance spectra measured between the current clinical system and each pixel of the FISI system. The spectra displayed are from phantom #14 and are calibrated to a reflectance standard and reference phantom. Overall there is reasonable agreement of the measured spectra between the clinical and FISI system. However, pixel #7 does show considerable deviation from all other measurements, particularly at the shorter wavelengths (400 and 420 nm).

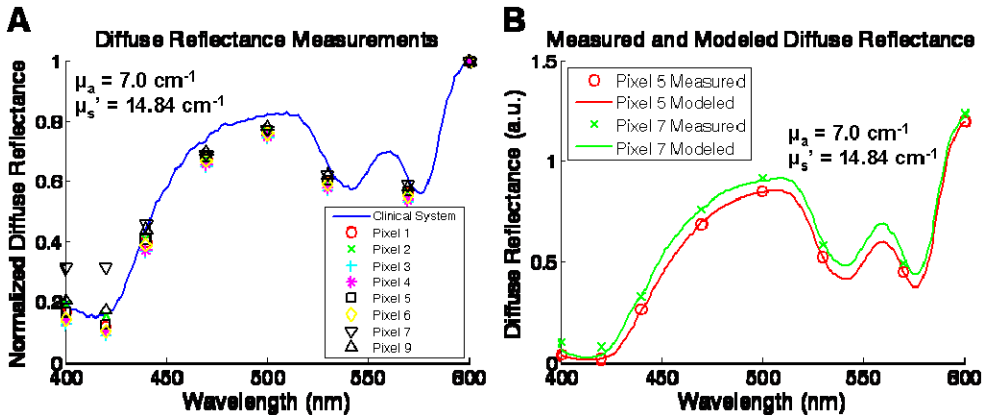

Figure 2.4: A) Calibrated reflectance spectrum collected from phantom 14 using the clinical and FISI system. B) Measured and modeled diffuse reflectance spectra from the FISI system.

Using the scalable inverse MC model, a modeled diffused reflectance spectrum was fitted to the measured spectrum to extract the optical properties of the sample. Figure 2.4B shows the measured spectrum and final modeled spectrum for two representative pixels (#5 and #7). While the measured and modeled spectra are in agreement for pixel #5, a small deviation exists between 400-420 nm in pixel #7. The inability to accurately model the spectra stems from the measurement error which may be is attributed to a construction defect present in pixel 7.

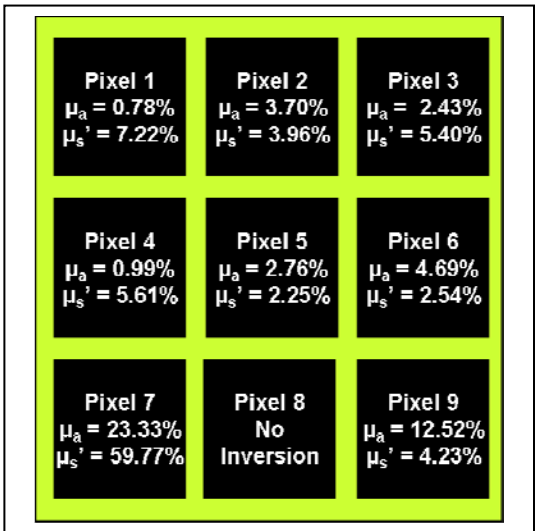

Figure 2.5: Summary of the optical property extraction errors for all pixels.

The percent error between the extracted optical properties and expected optical properties are calculated and summarized in Figure 2.5 for all pixels. A single value for error percentage is reported by taking the averaging over all wavelengths and all target phantoms. Most of the pixels (except pixel 7) are capable of extracting μ_a and μ_s' with high accuracy (<8% error).

Finally, a comparison of performance metrics between the current clinical system and FISI system are shown in Table 2.4. The uncertainty reported in the optical property extraction column is the standard deviation of error over all pixels and phantoms.

Table 2.4: Comparison of performance metrics between the clinical system and filter-photodiode system.

Spectral Imaging System	# wavelengths between 400-600 nm	Drift	SNR @ 600 nm (dB)	Absorption (μ_a) and Scattering (μ_s')	
				Mean μ_a Error	Mean μ_s' Error
Current Clinical System	**81**	**±3%**	**42**	**9.03%**	**7.33%**
Fiber-Illuminated System	**8**	**±2%**	**46**	**6.40±7.78%**	**11.37±19.62%**

These results with the FISI system demonstrate that the system is comparable with the current clinical system in terms of performance. However, replacing the grating-based spectrograph and CCD with an 8-slot filter wheel and 9 photodiodes immensely reduced both the footprint and cost of the system. In addition, experimentally demonstrating that with 8 wavelengths optical properties could still be accurately extracted was an important step toward the ultimate goal of replacing the light source. Rather than using a broadband light source with bandpass filters, it would be reasonable to investigate using multiple LEDs, at different discrete wavelengths, as the light source.

(c) Back-illumination Spectral Imaging (BISI) System

While the FISI system showed the potential for spectral imaging with performance in measuring tissue optical properties comparable to that of the current clinical system, fabrication of a larger imaging array could be challenging to deal with a large number of fibers and aligning all these fibers to flush with the detectors. On the other hand, the back illumination strategy completely obviates the need for fibers at the device-tissue interface. In the BISI system, the fiber bundle (Figure 2.2A) was replaced by a liquid light guide, as shown in Figure 2.6A. The light guide serves to deliver light from the source to a probe housing, in which the light diverges, and propagates in free space; a portion of the beam is transmitted through the apertures (holes) in each detector. The holes were sealed with biocompatible, transparent epoxy to prevent liquid from getting into the probe housing.

The BISI system uses the same Xe light source as the FISI system with 8 bandpass filters for illumination and a 4x4 array of 2.4x2.4 mm^2 silicon photodiodes with 1.0 mm holes in the center for detection. Light from the lamp is back-illuminated through the holes of the detectors, which are in contact with the tissue sample. Figure 2.6B is an image of the prototype created this year. The current prototype is a much more compact, fiber-less device that is even less costly.

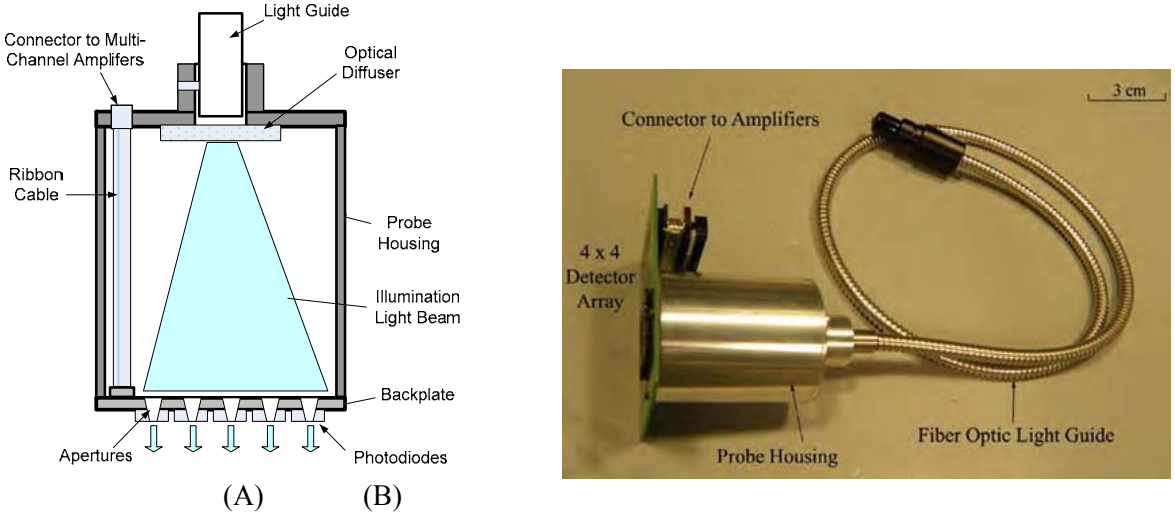

Figure 2.6: A) Schematic of the probe housing, showing the back-illumination strategy and (B) Image of the first BISI prototype

Due to the high cost of sophisticated phantom studies required to fully characterize the multi-pixel probes, a single-pixel version of the BISI probe was created to show proof of concept. The single-pixel probe is shown in Figure 2.7. A 1 mm diameter hole was drilled in the center of a 2.4x2.4 mm^2 silicon photodetector. The Xe lamp with 8 filters and a light guide was used to back-illuminate the probe. Hemoglobin and 1-μm polystyrene microspheres were used to create 15 phantoms over a wide range of optical properties similar to those of human breast tissue (average absorption coefficient = 1.3-10.3 cm^{-1} and average reduced scattering coefficient = 8-12 cm^{-1}). Again the scalable inverse MC model of reflectance was used to perform inversions to extract optical properties from the measured data. The overall average absorption extraction error was 8.4% and the average scattering extraction error was 3.6%. Plots of expected versus extracted optical properties are shown in Figures 2.8. These results show proof-of-concept that the back-illumination strategy with only 8 wavelengths can be used to extract optical properties with good accuracy. The device can be seamlessly multiplexed and shows feasibility for future use in quantitative spectral imaging of breast tissue.

Figure 2.7: Image of a single-pixel back-illuminated probe.

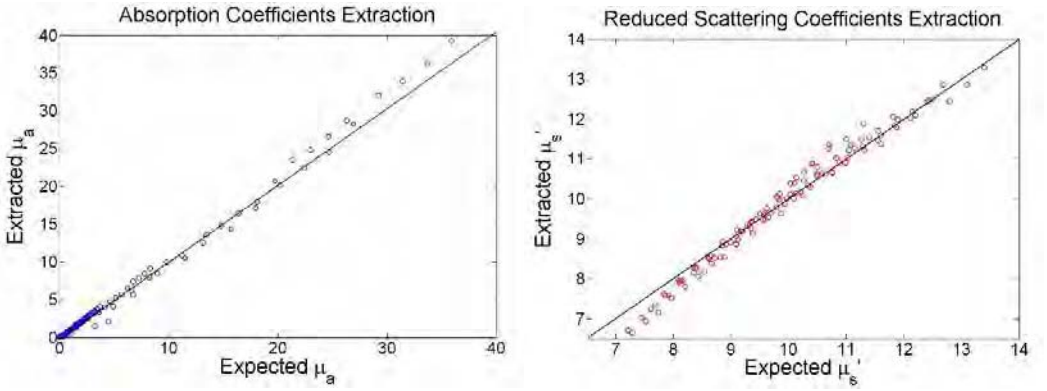

Figure 2.8: Extracted v.s. expected optical properties using the single-pixel back-illuminated device.

(d) GaAs Photodiode Fabrication

We have also made initial photodiode arrays using a GaAs technology through a process similar to the Si photodiode process proposed. This GaAs-based technology was used to test initial feasibility using in-house capabilities and experience. The arrays are shown in Figures 2.9(A) and (B). These diodes will have etched holes for the optical illumination, through the device, as proposed. The initial structures have demonstrated a strong detected signal using broadband illumination, with ~1.5 mA of current associated with the detected light as indicated in the measured dark and illuminated current-voltage (IV) characteristics (Figure 2.9(C)). This result demonstrated the in-house capability to develop and fabricate photodiode arrays with strong measured photocurrent.

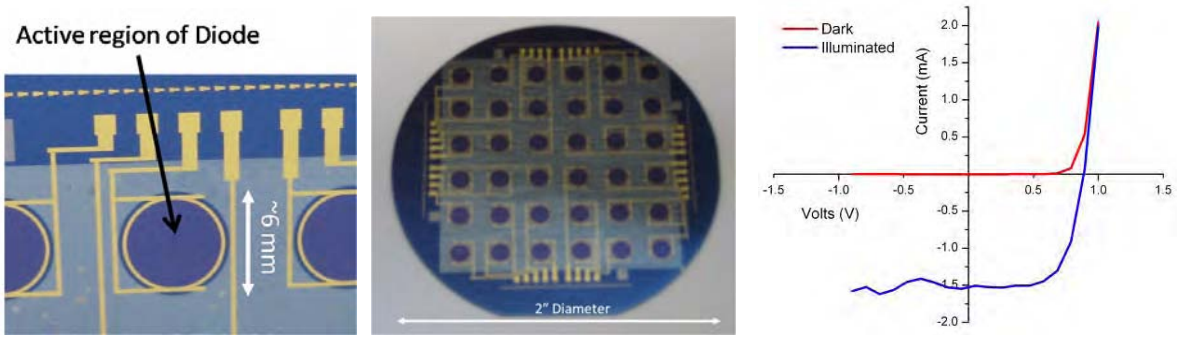

(A) (B) (C)

Figure 2.9: GaAs photodiodes: (A) details of a single-pixel; (B) initial 6x6 photodiode arrays; and (C) I-V characteristics.

F. Plans for years 5

- To complete development of the 4x4 BISI system.
- To test the FISI and BISI systems in the imaging mode using Intralipid phantoms.
- To fabricate and characterize a 6x6 ring-shaped GaAs photodiode array.
- To use the multi-pixel fiber-photodiode device to collect spectra from 5 – 10 ex-vivo lumpectomy specimens.
- To analyze the spectra data collected using the fiber-photodiode device and the BISI device.

3.1 Project 2: Exploiting, physiological, metabolic and molecular contrast in breast cancer

A. Original SOW for five years

1) *Physiological and metabolic characterization of mammary tumors in an animal model of breast cancer.* Nude mice will be injected in the flank with 500,000 4T1/D2 cancer cells. The tumors will be allowed to grow until they have reached a size of approximately 8 mm in diameter (approximately 1-2 weeks). Non-invasive optical measurements of tumor oxygenation, vascularity and metabolism will be measured using a continuous wave system and compared to independent measurements of tumor hypoxia using an OxyLite fiber optic sensor and immunohistochemistry of hypoxic and metabolic markers (year 1).
2) *Synthesis of contrast agents for molecular imaging.* Gold nanoparticles will be prepared via citrate reduction of chloroauric acid. The particle size will be adjusted to preferentially scatter NIR light. Anti-HER2 and anti-EGFR antibodies will be conjugated to the gold. The scattering spectrum of (1) the pre-labeled nanoparticles will be measured to verify their NIR resonant scattering properties and (2) the labeled nanoparticles to verify binding with the antibodies (a characteristic red-shift in the peak is expected to occur after binding) (year 2).
3) *Molecular imaging in cells*. Human breast cancer cell lines, MDA-MB-468 and SK-BR-3 which over express EGFR and HER2, respectively will be cultured to test the targeting strategies. Cell lines that express low levels of EGFR and HER2 will be used as controls. Each cell type will be labeled according to previously established protocols and imaged using a microscope coupled to a CCD camera. The optical contrast in the cells over expressing HER2 and EGFR receptors relative to that in the control cells will be statistically compared to demonstrate the molecular specificity of the anti-EGFR and anti-HER2 nanoparticles (year 3).
4) *Molecular imaging in animal models.* Tumor cell lines will be stably transfected to over express both HER2 and EGFR, and tumors will be grown in the mammary fat pad of the nude mice used in (a). Both topical and systemic injection of the molecular contrast agents will be explored. An optical imaging system consisting of a tunable laser and a CCD camera will be used to image the molecularly tagged contrast agents for different doses (to measure the effect of dosimetry on the signal to background) as well as for topical vs. systemic delivery. Note that task (a) is directly relevant to this aim as it will provide the instrumentation and algorithms for data analysis as well as experience with the preparation of animal tumor models for these studies (years 4-5).

The original project proposed here has evolved into two distinct projects: (1) The development of techniques to exploit the intrinsic sources of optical contrast (physiologic and morphological) as a means to assess response to cancer therapy and (2) the assessment of extrinsic sources of optical contrast for use as an aid in intra-operative assessment of breast tumor margins.

B. Summary of Accomplishments in years 1 and 2

The goal of this year 1 study was to quantify and track changes in oxygenation in response to carbogen breathing in 4T1 breast tumors in nude mice using optical spectroscopy. Specifically we measured hemoglobin saturation and the optical redox ratio and compared the optical measures of oxygenation to that of a well established method of measuring tumor pO_2, the OxyLite system, to demonstrate the utility of optical spectroscopy to quantitatively monitor tumor physiology in a pre-clinical model.Non-invasive optical spectroscopy was performed on 4T1 breast tumors grown in the flank of nude mice (n=10) before and after the administration of carbogen (95% O2, 5% CO2), by placing a fiber optic probe in contact with the surface of the tumor.

This work established the ability of optical spectroscopy to consistently track changes in tumor physiology in response to a perturbation. It was found that optical spectroscopy may in fact provide a

more robust assessment of tissue oxygenation than the existing Oxylite system, likely due to its larger probing volume. This work establishes optical spectroscopy as a viable tool to monitor changes in tumor physiology in response to other treatments, including radiation, chemotherapy, and molecular therapies, offering many advantages over existing technologies. In particular, it is fast, non-invasive, quantitative, and probes a wide range of physiologic parameters, including blood content, oxygenation, and cellular metabolism. This project has subsequently expanded and will span the full five years of the proposal.

C. Summary of Accomplishments in year 3

Establishing the validity of intrinsic optical biomarkers to quantitatively and longitudinally monitor tumor hypoxia and necrosis in murine tumor models:
Diffuse reflectance spectroscopy was evaluated as a objective tool to assess quantitative physiological changes in solid murine tumor models when exposed to chemotherapy. Specifically, it was investigated whether the optical technique could assess changes in tumor hypoxia and necrosis relative to the traditional immunohistochemical methods. N=50 nude mice were inoculated with 4T1 mouse breast carcinoma cells on their flanks and were evenly distributed into control and treatment groups (each group had 25 animals). The treatment group received an 10 mg/kg of Doxorubicin while the control group received an equivalent volume of saline. The tumors were monitored optically prior to treatment and then for 2 weeks post treatment. Five randomly chosen animals, from each group, were removed for immunohistochemical (IHC) analysis on 4 different days. We found that the optical markers of de-oxygenated hemoglobin and the wavelength-averaged optical tissue scattering coefficient were directly correlated to immunohistochemical assessment of tumor hypoxia and histologically estimated tumor necrosis, respectively. Further we established that the temporal trends in these optical and immunohistochemical parameters were concordant with one another. Another result from this study was that optical measurements indicated a clear and statistically significant increase in the oxygen content in the treated tumors relative to the untreated animals, while both immunohistochemical and tumor growth delay assays showed no differences between the treatment and control groups, lending further credence to the fact that such non-invasive methods may provide both better and earlier indications of treatment effects.

Molecular imaging with 5-ALA:
The research goals for year 3 have changed from the synthesis of scattering contrast agents that was originally proposed to detecting mammary cancer with fluorescent contrast agents. Fluorescence agents were chosen over scattering contrast agents because fluorescence has a unique excitation and emission. In the previous year, aminolevulinic acid (ALA) induced protoporphyrin IX (PpIX) was successfully used to differentiate cancerous cells from normal with fluorescence lifetime. This work was carried on into the beginning of this year by examining fluorescence intensity and spectroscopy. It was found that PpIX has a significantly greater fluorescence increase in malignant cells as compared to normal cells. However, the raw fluorescence intensity of cells cannot be used to delineate malignant from normal without a fluorescence control to determine the endogenous fluorescence. The long incubation time, 2 hours, and endogenous fluorescence required to detect PpIX is clinically prohibitive. It was concluded that for clinical use within the operating room, PpIX is not ideal.

D. Progress Report for year 4

Using optical spectroscopy to assess early response to radiotherapy using intrinsic optical biomarkers

Introduction: The currently accepted standard practice to assess the efficacy of anti-cancer treatments in preclinical studies uses the tumor growth delay assay. Though useful, the uni-dimensional measurements of tumor volume hide a plethora of functional, physiological and

metabolic information regarding how the tumors are responding toward treatments. Further, relying solely on tumor growth/recurrence to indicate treatment response requires a long period of sustained observations. We wanted to evaluate if diffuse reflectance spectroscopy could be used as an objective tool to assess early response in solid murine tumors model that were exposed to radiotherapy. The non-invasive and quantitative nature of this technique along with its ability to performed using a variety of different fiber-optic probe geometries makes it highly relevant to translational applications. We have completed a preliminary animal study to explore the feasibility of using optical biomarkers obtained early during a course of curative radiotherapy in predicting long term local tumor control.

Study Design: N=34 nude mice were inoculated with 10^6 FaDu human hypopharyngeal squamous cell carcinoma cells, subcutaneously, on their right flanks. Once the average tumor diameters reached 6-8 mm, the animals were evenly distributed by tumor volume into control and treatment groups in a 1:2 ratio, respectively. N=23 animals in the treatment group were exposed to 39 Gy of radiation, while N=11 animals in the control group received sham irradiation. The dose of 39 Gy was chosen as it has previously been reported as the TCD_{50} (dose which provides local control to 50% of the treated population) for this tumor model in nude mice. Treatment day was labeled day 0. All tumors were monitored optically before treatment to get baseline measurements on day 0 and then again on days 1, 3, 5, 7, 10, 12, 14 and 17. Tumor volumes were measured once using calipers each day over the course of the optical measurements and then one or two times per week until 120 days post treatment.

Results: This study was one of the first of its kind to demonstrate the predictive ability of a non-invasive sensing method to select animals that had complete local control relative to animals that fail treatment. We observed that animals showing complete local control (as defined by the lack of a palpable/visible lesion 120 days post treatment) showed statistically significant rates of increase in tumor oxygen saturation as early as 7 days post-irradiation, relative to the subjects that failed treatment. These responding animals also maintained higher levels of tumor oxygen saturation relative to the animals that failed treatment up to 17 days post-treatment. We have been able to build preliminary linear discriminant models that were able to separate the animals that responded to the treatment vs. not with 100% sensitivity and 85% specifity.

Plans for year 5: Given the promising results we obtained from our preliminary measurements of using diffuse optical methods to predict long term local control in irradiated murine tumor models, we will explore the applicability of the optical methods to predict treatment outcome in additional cell lines. Further, our initial study used a radiation dosimetry scheme that is seldom used clinically. In the studies for year 5, we will test the ability of optical methods to predict treatment outcome in murine tumors when they are irradiated using a fractionated schedule, to make them more relevant to clinically accepted radiation treatments.

Molecular imaging with NBDG

Introduction: The breast is highly heterogeneous with differing phenotypes, which creates issues in finding applicable molecularly specific contrast agents. Our previous work focused on ALA. ALA leveraged on changes in the heme pathway that are ubiquitous across cancers. Another potential universal contrast agent is 2-[*N*-(7-nitrobenz-2-oxa-1,3-diazol-4-yl)amino]-2-deoxy-D-glucose (2-NBDG). 2-NBDG is a fluorescent glucose analog and accumulates in cancerous cells that have high rates of glycolysis and rely on glucose for energy more than normal cells. 2-NBDG utilizes glucose transporters (GLUT) to cross the cellular membrane, is phosphorylated by hexokinases (HK), cannot be further metabolized and accrues in the cell. 2-NBDG is excited between 400-500 nm and emits at 540 nm. Previous studies have demonstrated 2-NBDG uptake in mammary cancer cells in less than 30 minutes. The short incubation period and cancer specificity makes 2-NBDG a suitable alternative to ALA. Our studies examine a large panel of breast cancer

cell lines with varying receptor statuses and demonstrate the potential of 2-NBDG in monitoring cellular response to therapy.

Study Design: Eight plates were incubated with 200 uM of 2-NBDG in media or media only control (4 in 2-NBDG, 4 control) in the following 10 breast cell lines of varying receptor statuses (Table 3.1).

Table 3.1: Summary of cell lines tested and the ER, HER2 and PR receptor status

Cell Line	Type	ER	HER2	PR
MCF12	Normal			
HMEC	Normal			
BT-474	Malignant	+	+	+
T47D	Malignant	+	-	+
MCF7	Malignant	+	-	+
MDA-MB-435	Malignant	-	-	-
BT-20	Malignant	-	-	-
MDA-MB-361	Malignant	+	+	-
MDA-MB-231	Malignant	-	-	-
MDA-MB-468	Malignant	-	-	-

Fluorescence intensity was measured on a Leica SP5 confocal microscope and quantified in ImageJ to determine the change in fluorescence between 2-NBDG incubated and control plates. The relative protein expression of GLUT 1 and HK I was determined following Western blot analysis. Finally, a subset of cell lines (MDA-MB-435 and MDA-MB-468) were treated with lonidamine (which decreases glycolysis by inhibiting phosphorylation) or alpha-cyano-hydroxycinnamate (which increases glycolysis by inhibiting cellular lactate uptake and usage).

Results: The preliminary results quantified the relative change in 2-NBDG and all cells demonstrated an uptake of 2-NBDG, but the HMEC normal mammary epithelial cell line was significantly less fluorescent than all other cell lines. HMEC did not express GLUT1, the most commonly expressed GLUT, and it is believed to be the cause of the lack of uptake. HK I, a mitochondrial bound enzyme that phosphorylates 2-NBDG, was expressed in all cell lines. Direct inhibition of HK I with the pre-clinical chemotherapeutic agent, lonidamine (LND) in the subset of cells was shown to decrease 2-NBDG uptake ($p<0.05$). Thus, the importance of GLUT1 and HKI for the accumulation of 2-NBDG was established as well as the ability to measure glycolytic inhibition. Finally, the pre-clinical cancer therapy, a-cyano-4-hydroxycinnamate (a-Cinn), which causes cells to increase glycolysis, was used to treat the same subset of cells. The a-Cinn treated cells had increased 2-NBDG uptake ($p<0.01$). This demonstrates great potential as a method to monitor changes in cancer cell glycolysis caused by therapy and will be further explored in animal models.

Plans for year 5: In Year 5, we will employ the use of a murine window chamber model to evaluate the distribution of 2-NBDG within a tumor. The 4T1-RFP (red fluorescent protein) mouse mammary tumor line will be implanted in window chambers surgically installed into the dorsal flap of mice. From these findings, we hope to visualize the distribution of 2-NBDG throughout a tumor as well as the hemoglobin saturation of the tumor tissue to be able to compare uptake and vasculature. This will be examined real-time on an *in vivo* hyperspectral microscope. During initial investigations, the proper dosage and optimal imaging time will be determined. Then, in a second set of window chamber mice, the response of tumors to glycolytic inhibition and stimuli will be examined. The inhibition will be induced by lonidamine, which was shown be effective in Year 4 on breast cancer cell lines. Glycolytic stimuli will be induced by a-Cinn, which was found to be effective on cancer cells in Year 4 as well.

4. KEY RESEARCH ACCOMPLISHMENTS

Project 1. System-on-a-chip device

- Construction of the 3x3 fiber-based illumination spectral imaging (FISI) array.
- The 3x3 FISI array was tested in liquid tissue-simulating phantoms using a new xenon light source with eight bandpass filters as the light source (simulating reduced number of wavelength).
- A single-pixel version of the back-illuminated spectral imaging (BISI) probe was built and tested in liquid tissue-simulating phantoms.
- The single-pixel BISI probe was expanded to a 4x4 array for spectral imaging.
- Initial photodiode arrays using a GaAs technology were fabricated and characterized. With the custom GaAs array and the back-illumination strategy, a miniature spectral imaging system can be built with the application for intra-operative assessment of tumor margins.

Project 2. Exploiting, physiological, metabolic and molecular contrast in breast cancer

- Longitudinal measurements of tumor physiology using optical biomarkers provide early estimates of changes in tumor oxygenation patterns in irradiated tumors.
- Rapid and sustained reoxygenation in irradiated tumors indicates better probability for long term local tumor control in irradiated tumors.
- Optical biomarkers may be able to predict long-term treatment outcomes as early as 1-2 weeks after treatment initiation.
- 2-NBDG was taken up significantly in a panel of breast cancer cell lines regardless of phenotype and receptor status (estrogen receptor, human epidermal growth receptor 2+ and progesterone receptor were all varied).
- 2-NBDG metabolism was inhibited with lonidamine, which prevented phosphorylation of 2-NBDG and ultimately accumulation as shown by fluorescence intensity changes in uptake after treatment.
- Glycolysis was increased by treating cells with alpha-hydroxycinnamate and subsequent uptake of 2-NBDG was increased.

5. REPORTABLE OUTCOMES

Project 1. System-on-a-chip device

1) Yu B, Lo JY, Palmer GM, Bender J, Kuech TF, Ramanujam N, “A Cost-Effective Diffuse Reflectance Spectroscopy Device for Quantifying Tissue Absorption and Scattering *In Vivo*,” Journal of Biomedical Optics. 13 (6): 060505, 2008.
2) Lo JY, Yu B, Fu HL, Bender JE, Palmer GM, Kuech TF, Ramanujam N. A strategy for quantitative spectral imaging of tissue absorption and scattering using light emitting diodes and photodiodes. *Optics Express*. 17 (3):1372-1384, 2009.
3) Fu HL, Yu B, Lo JY, Palmer GM, Keuch T, Ramanujam N. "A Reduced-Cost Spectral Imaging System for Breast Tumor Margin Assessment." Advances in Optics for Biotechnology, Medicine, and Surgery XI. Burlington, VT, USA. June 2009 (Poster Presentation)

Project 2. Exploiting, physiological, metabolic and molecular contrast in breast cancer

1) Millon SR, Ostrander JH, Brown JQ, Ramanujam N. "Uptake of 2-NBDG in normal mammary epithelial and breast cancer cells." ECI (2009).
2) Millon SR, Ostrander JH, Brown JQ, Ramanujam N. "2-NBDG for use in breast cancer detection and therapy monitoring in vitro." Fitzpatrick Symposium: Frontiers in Photonics and Science (2009).
3) Millon SR, Ostrander JH, Brown JQ, Ramanujam N. "2-NBDG for use in breast cancer detection and therapy monitoring in vitro." Duke Comprehensive Cancer Center Annual Meeting. (2009).
4) Vishwanath K, Huan Y, Barry WT, Dewhirst MW, and Ramanujam N. Using Optical Spectroscopy to Longitudinally Monitor Physiological Changes within Solid Tumors. *Neoplasia* **11**, 889-900. 2009
5) Vishwanath K, Klein D, Chang K, Schroder T, Dewhirst M, and Ramanujam N. Quantitative optical spectroscopy can identify long term local control in irradiated murine head and neck xenografts. *J Biomed Opt* 14(5), 054051. 2009

6. CONCLUSIONS

A. Project 1

In year 3, we have modified the probe geometries of the single-pixel probe developed in year 2 in order to increase the signal-to-noise ratio of the probe and to be able to extract a much larger range of optical properties than those of the probes built in year 2. The new probe was tested in synthetic tissue phantoms over a wide range of absorption and reduced scattering coefficients, and the phantom optical properties were extracted from the diffuse reflectance spectra obtained from the tunable light source and new probe with the inverse MC model previously developed by our group. Using the same phantom data collected by our new probe, optical properties with a reduced number of wavelengths were extracted to assess the feasibility of replacing the tunable light source with several smaller LEDs to further reduce the size and cost of the current system. In addition, cross-talk analysis was performed as a first step to multiplex the single pixel system into an imaging system that can quantify tissue physiological and morphological properties over a large tissue area. We have also fabricated a 3x3 fiber-photodiode array for test in the lab.

In year 4, the single-pixel probe (using a 5.8x5.8 mm Si detector) with fiber-based illumination developed in year 3 have been expanded to a 3x3 spectral imaging (FISI) array. A FISI system was constructed using the 3x3 array and an 8-wavelength xenon light source. The FISI system was tested in a number of homogeneous liquid phantoms with optical properties representative of breast tissue and excellent accuracy was achieved in extraction of the phantom optical properties. This demonstrated the possibility of performing spectral imaging with low cost photodiodes and 8 LEDs covering the wavelength range from 400 – 600 nm. To further reduce the size and cost and to simplify the probe fabrication, we have proposed a new back-illumination strategy to replace the fiber-based illumination. A single-pixel version of the back-illuminated probe (using a 2.4x2.4 mm Si detector) was built and tested and the performance was found to be comparable to those of the FISI array and the current clinical system. A 4x4 back-illuminated spectral imaging (BISI) array has also been designed and the optimization and testing will be performed in year 5. The drilled commercial Si detectors are good for proof-of-concept study, but our long term goal is to build a system-on-a-chip spectral imaging device, which requires the integration of photodiodes, light delivery network and electronics on to a single wafer. In year 4, we have also made initial GaAs photodiode arrays that will be improved and optimized in year 5.

B. Project 2

a. Molecular imaging with NBDG

In the previous year, a large panel of breast cancer cell lines of varying receptor types and normal mammary epithelial cells were tested to determine a) metabolic protein expression b) baseline 2-NBDG uptake c) 2-NBDG uptake after a decrease and increase in glycolysis with lonidamine and alpha-hydroxycinnamate, respectively. The cell line with a lack of GLUT 1 expression failed to show 2-NBDG uptake. Furthermore, inhibition of HK I and resulting inhibition of glycolysis with lonidamine decreased 2-NBDG uptake ($p<0.05$) and, alpha-cyano-hydroxycinnamate caused cells to increase glycolysis and subsequent 2-NBDG uptake in the same subset of breast cancer cells ($p<0.01$). This demonstrates potential of NBDG as a method to monitor differences in glycolysis and will be further explored in cell and animal models.

b. Assessing treatment outcome using optical spectroscopy

In year 4, we specifically tested whether a sequence of longitudinal optical spectroscopic measurements obtained for up to two weeks post-radiotherapy could predict for long term loco-regional control in one human squamous cell carcinoma cell line, in a nude mouse model. The results from this preliminary study established (a) that optical spectroscopy can provide a useful, non-invasive and simple means to monitor perturbations in tumor physiology as a function of treatment, (b) that there were significant differences in the patterns of tumor oxygenation following treatment in individual subjects, and (c) that the trends in tumor oxygenation could statistically significantly ($p < 0.01$) discriminate between animals that showed local control vs. those that failed treatment, as early as 7 days post treatment. We intend to further explore the validity of optical methods in predicting early treatment response to radiotherapy in future studies by: (i) using a fractionated radiation treatment schedule to better reflect clinically followed treatment schedules, and (ii) testing additional cancer cell lines.

7. REFERENCES

1. Yu, B. and N. Ramanujam, *A Cost-Effective Diffuse Reflectance Spectroscopy Device for Quantifying Tissue Absorption and Scattering In Vivo.* Opt Lett, 2008.
2. Zhu, C., Palmer GM, Breslin TM, Harter JM, Ramanujam N, *Diagnosis of Breast Cancer using Fluorescence and Diffuse Reflectance Spectroscopy: a Monte Carle Based Approach.* J Biomed Opt, 2008. **13**(3): p. 034015.
3. Prahl, S., *Mie scattering program*. 2005, Oregon Medical Laser Center, available at http://omlc.ogi.edu/software/mie/index.html.
4. Chan, E.K., B. Sorg, D. Protsenko, M. O'Neil, M. Motamedi, and A.J. Welch, *Effects of compression on soft tissue optical properties.* Selected Topics in Quantum Electronics, IEEE Journal of, 1996. **2**(4): p. 943 - 950